



HAL
open science

A fast H₂O total column density product from GOME? validation with in-situ aircraft measurements

T. Wagner, J. Heland, M. Zöger, U. Platt

► **To cite this version:**

T. Wagner, J. Heland, M. Zöger, U. Platt. A fast H₂O total column density product from GOME? validation with in-situ aircraft measurements. Atmospheric Chemistry and Physics Discussions, 2003, 3 (1), pp.323-353. hal-00300872

HAL Id: hal-00300872

<https://hal.science/hal-00300872>

Submitted on 18 Jun 2008

HAL is a multi-disciplinary open access archive for the deposit and dissemination of scientific research documents, whether they are published or not. The documents may come from teaching and research institutions in France or abroad, or from public or private research centers.

L'archive ouverte pluridisciplinaire **HAL**, est destinée au dépôt et à la diffusion de documents scientifiques de niveau recherche, publiés ou non, émanant des établissements d'enseignement et de recherche français ou étrangers, des laboratoires publics ou privés.

A fast H₂O total column density product from GOME

T. Wagner et al.

A fast H₂O total column density product from GOME – validation with in-situ aircraft measurements

T. Wagner¹, J. Heland², M. Zöger³, and U. Platt¹

¹Institut für Umweltphysik, University of Heidelberg, Germany

²Deutsches Zentrum für Luft- und Raumfahrt (DLR), Institut für Physik der Atmosphäre, Oberpfaffenhofen, Germany

³Deutsches Zentrum für Luft- und Raumfahrt (DLR), Flugabteilung, Oberpfaffenhofen, Germany

Received: 31 October 2002 – Accepted: 9 January 2003 – Published: 29 January 2003

Correspondence to: T. Wagner (thomas.wagner@iup.uni-heidelberg.de)

[Title Page](#)

[Abstract](#)

[Introduction](#)

[Conclusions](#)

[References](#)

[Tables](#)

[Figures](#)

[⏪](#)

[⏩](#)

[◀](#)

[▶](#)

[Back](#)

[Close](#)

[Full Screen / Esc](#)

[Print Version](#)

[Interactive Discussion](#)

© EGU 2003

Abstract

Atmospheric water vapour is the most important greenhouse gas which is responsible for about 2/3 of the natural greenhouse effect, therefore changes in atmospheric water vapour in a changing climate (the water vapour feedback) is subject to intense debate.

H₂O is also involved in many important reaction cycles of atmospheric chemistry, e.g. in the production of the OH radical. Thus, long time series of global H₂O data are highly required. Since 1995 the Global Ozone Monitoring Experiment (GOME) continuously observes atmospheric trace gases. In particular it has been demonstrated that GOME as a nadir looking UV/vis-instrument is sensitive to many tropospheric trace gases.

Here we present a new, fast H₂O algorithm for the retrieval of vertical column densities from GOME measurements. In contrast to existing H₂O retrieval algorithms it does not depend on additional information like e.g. the climatic zone, aerosol content or ground albedo. It includes an internal cloud-, aerosol-, and albedo correction which is based on simultaneous observations of the oxygen dimer O₄. The high accuracy of our GOME H₂O data is confirmed by the excellent agreement with in-situ aircraft measurements during the MINOS campaign in Greece in summer 2001. Our H₂O algorithm can be directly adapted to the nadir observations of SCIAMACHY (SCanning Imaging Absorption SpectroMeter for Atmospheric CHartography) which was launched on ENVISAT in March 2002. Near real time H₂O column data from GOME and SCIAMACHY might be of great value for meteorological weather forecast.

1. Introduction

Global data sets of atmospheric H₂O are needed for the investigation of important atmospheric processes. As the most important atmospheric greenhouse gas H₂O is strongly involved in the energy balance of the earth's atmosphere. An increase of the atmospheric temperatures should result in higher evaporation rates and thus could cause increased atmospheric water vapour contents, e.g. leading to higher precipita-

A fast H₂O total column density product from GOME

T. Wagner et al.

Title Page

Abstract

Introduction

Conclusions

References

Tables

Figures

⏪

⏩

◀

▶

Back

Close

Full Screen / Esc

Print Version

Interactive Discussion

A fast H₂O total column density product from GOME

T. Wagner et al.

[Title Page](#)[Abstract](#)[Introduction](#)[Conclusions](#)[References](#)[Tables](#)[Figures](#)[◀](#)[▶](#)[◀](#)[▶](#)[Back](#)[Close](#)[Full Screen / Esc](#)[Print Version](#)[Interactive Discussion](#)

© EGU 2003

tion rates. Long term global data sets might be well suited to investigate whether such an increase of the atmospheric water vapour content has already taken place. Near real time GOME H₂O column data over extended areas might also serve as valuable input to improve meteorological weather forecast. In particular they could be helpful in predicting heavy precipitation events.

H₂O also plays an important role in many atmospheric chemical reactions. In the troposphere the reaction of O(¹D) with H₂O is the dominant source for the OH radical which is the most important atmospheric reactant (see e.g. Atkinson, 1990, 2000).

For these reasons extended global data sets of the atmospheric H₂O distribution are highly required. H₂O has so far been measured by in-situ observations with hygrometers at the ground, on radiosondes and on aircraft. Remote sensing from the ground is usually performed with spectroscopic methods using photometers. Such observations yield the integrated atmospheric H₂O concentration, the so called vertical column density, VCD in units of molec./cm⁻² (Halthore et al., 1997). However, both the in-situ and photometer measurements can only provide local information. For the determination of the global atmospheric H₂O distribution satellite observations are necessary. Several satellite instruments, e.g. MLS, HALOE, SAGE II, POAM, LIMS, ATMOS, MAS, and ILAS yield H₂O concentration profiles in the stratosphere by solar occultation or microwave limb emission techniques. A good overview and summary can be found in Kley and Russel (2001). However, information on the H₂O content of the middle or lower troposphere could not be retrieved from these observations.

First global tropospheric H₂O data from satellite measurements have been analysed from TOVS and GOES measurements (Jedlovec, 1987; Soden and Bretherton, 1996; Chaboureau et al., 1998; references therein). They yielded (limited) information on the vertical distribution but lacking precise information on the total atmospheric H₂O column. Observations of upper tropospheric H₂O in the IR spectral region were also performed by the CRISTA instrument on board the NASA Space shuttle (Schaeler and Riese, 2001).

Tropospheric H₂O data are also obtained from microwave observations of the Spe-

cial Sensor Microwave Imager (SSM/I) (Bauer and Schuessel, 1993). Recently, atmospheric H₂O data have also been derived from the signals of the GPS network (Bevis et al., 1992; Rocken et al., 1997; Baltink et al., 2002). This new and very promising method utilizes the influence of atmospheric H₂O on the GPS signals. Most recently global GPS water vapour profiles could be obtained from the CHAMP satellite (Wickert et al., 2001).

In April 1995 the Global Ozone Monitoring Experiment (GOME) was launched on ERS-2. As a nadir-looking-UV/vis-instrument GOME is capable of measuring several tropospheric trace gases like NO₂, BrO, HCHO, SO₂, H₂O and O₃ (ESA, 1995). In particular it can observe the total atmospheric H₂O column including the layers near the surface. GOME is now continuously operating for more than 7 years, thus these observations might be well suited for the investigation of trends of atmospheric trace gases like H₂O. Atmospheric H₂O has already been analysed from GOME observations and compared to independent data sets by different groups (Noël et al., 1999; Maurellis et al., 2000; Casadio et al., 2000; Noël et al., 2000, 2002; Lang et al., 2002) and reasonable agreement was found. However, these GOME H₂O algorithms suffer from different shortcomings:

- a) First, they are based on complex retrieval schemes including e.g. different reference atmospheres (see e.g. Noël et al., 1999) or vertically resolved atmospheric modelling (see e.g. Lang et al., 2002). Such complex retrieval schemes might be appropriate if sufficient information on the atmospheric properties during the measurements is available. However, this is usually not the case for the large amount of GOME observations.
- b) Second, these algorithms typically mix information from the measurements with additional information like assumptions on the atmospheric aerosol content, ground albedo and radiative transfer (see e.g. Lang et al., 2002). Thus the H₂O results become dependent not only on the observations but also on this a-priori information.
- c) Since most of the GOME observations are covered by clouds, the largest uncertainty of tropospheric trace gas products is due to the influence of clouds on the observed spectra. The earlier H₂O algorithms did not take this cloud influence into account at

A fast H₂O total column density product from GOMET. Wagner et al.

[Title Page](#)[Abstract](#)[Introduction](#)[Conclusions](#)[References](#)[Tables](#)[Figures](#)[◀](#)[▶](#)[◀](#)[▶](#)[Back](#)[Close](#)[Full Screen / Esc](#)[Print Version](#)[Interactive Discussion](#)

A fast H₂O total column density product from GOME

T. Wagner et al.

[Title Page](#)[Abstract](#)[Introduction](#)[Conclusions](#)[References](#)[Tables](#)[Figures](#)[◀](#)[▶](#)[◀](#)[▶](#)[Back](#)[Close](#)[Full Screen / Esc](#)[Print Version](#)[Interactive Discussion](#)

© EGU 2003

all. First very promising attempts for a cloud correction using O₂ absorptions were undertaken by Noël et al. (2000, 2002) and Casadio et al. (2000). However, usually the atmospheric profiles of O₂ with a scale height of ≈ 8 km and H₂O are quite different (see Sect. 2.3.3 and Fig. 1).

5 In this study we present a new H₂O retrieval algorithm from GOME observations which is based on the DOAS-method (e.g. Platt et al., 1994). It is shown that this spectral retrieval procedure is robust, very fast and in particular independent from assumptions on atmospheric properties. The saturation effect of the GOME H₂O observations is corrected for after the spectral retrieval. For this purpose a simple relationship between GOME observations and the atmospheric H₂O column density is used which is
10 derived from spectral convolution of the high resolved H₂O absorption structure with the instrument function of GOME (see e.g. Van Roozendael et al., 1999).

Finally the derived H₂O absorptions are converted into the atmospheric vertical column density using the simultaneously measured absorption of the oxygen dimer O₄. The vertical column density of O₄ is known – it varies slightly with changes in air density and can be expected to be nearly constant – therefore the GOME observations of O₄ allow the quantification of the effects of the atmospheric radiative transfer. This method has several advantages:

A) Since the O₄ concentration is proportional to the square of the oxygen concentration, the maximum of the O₄ concentration is located close to the Earth's surface with a scale height of about 4 km. Thus the effects of the radiative transport through the atmosphere are more similar to H₂O, which is also located close to the Earth's surface (see Fig. 1).

B) The effects of a changing ground albedo and aerosol content are largest for trace gases which are located close to the Earth's surface. The simultaneously measured O₄ absorption allows a direct correction for these influences without further independent assumptions.

C) Since clouds strongly influence the atmospheric radiative transfer and cover nearly all GOME pixels, an adequate cloud correction is the prerequisite for correct tropo-

A fast H₂O total column density product from GOME

T. Wagner et al.

[Title Page](#)[Abstract](#)[Introduction](#)[Conclusions](#)[References](#)[Tables](#)[Figures](#)[◀](#)[▶](#)[◀](#)[▶](#)[Back](#)[Close](#)[Full Screen / Esc](#)[Print Version](#)[Interactive Discussion](#)

© EGU 2003

spheric data products from GOME observations. In particular “subtle” cloud effects like multiple scattering inside clouds or horizontal light paths within the large ground pixels – which are difficult to model – are automatically taken into account.

D) No atmospheric radiative transfer modelling is included. In addition, all atmospheric scenes are analysed with the same retrieval approach. This makes our data analysis very transparent and stable.

The shortcomings of our approach include the remaining differences of the atmospheric radiative transfer for H₂O and O₄ and are caused by the differences of the altitude profiles and the differences in the absorption strength. However, for most of the GOME observations these differences are small. The high accuracy of our GOME H₂O data retrieval is confirmed by the excellent agreement with in-situ aircraft measurements during the MINOS campaign in Greece in summer 2001.

2. Instruments and data analysis

2.1. In-situ aircraft measurements of water vapour

The DLR research aircraft Falcon is permanently equipped with a standard in-situ meteorological measurement system to determine temperature, pressure, wind and humidity of the undisturbed air. The atmospheric water vapour is measured by three different instruments: a commercial aircraft dew point hygrometer (GE 1011B, General Eastern), a slightly modified capacitive sensor (Humicap-H®, Vaisala) and a Lyman-alpha absorption instrument (Buck Research, Boulder). The details of the instruments and intercomparisons with other sensors on board of different aircraft are described elsewhere (e.g. Buck, 1985; Ström et al., 1994; Helten et al., 1998).

Due to its fast response time of a few milliseconds and wide sensitivity range the data of the Lyman-alpha instrument are used whenever possible. At high boundary layer water vapour concentrations, where saturation of the Lyman-alpha absorption instrument occurred, the Humicap data were used. Covariance analysis of Humicap

A fast H₂O total column density product from GOMET. Wagner et al.

[Title Page](#)[Abstract](#)[Introduction](#)[Conclusions](#)[References](#)[Tables](#)[Figures](#)[⏪](#)[⏩](#)[◀](#)[▶](#)[Back](#)[Close](#)[Full Screen / Esc](#)[Print Version](#)[Interactive Discussion](#)

© EGU 2003

and Lyman-alpha time series yield a response time of 3 s for the Humicap instrument at boundary layer conditions. At typical ascent or descent rates of 8 m/s (1500 ft/min) this corresponds to a vertical resolution of approximately 25 m. The accuracy of this instrument under lower tropospheric conditions is better than 5%. Both instruments were calibrated with a calibration bench similar to the one described by Zöger et al. (1999) using a commercial frost/dew point hygrometer as reference. All calibrations were performed over a realistic range of water vapour concentrations and pressures and are traceable to national standards. The error of the calibration is less than 3% of the measured value.

The low time resolution of the aircraft dew point hygrometer yielded a very low data coverage. Thus useful data of the dew point hygrometer were used only for consistency check with the other instruments.

In order to reduce the amount of data the experimental data were averaged in 100 m altitude bins. In addition, since the error of the Lyman-alpha instrument is a non-linear function of the water vapour concentration and the pressure, a dedicated error analysis for the sensors was performed along the flight track of a representative flight, and averaged into 100 m altitude bins, too. Figure 2 shows the altitude profile of MINOS flight # 6 on 14 August 2001 (Fig. 2a), the variability of the data in the 100 m bins as 1σ standard deviations (Fig. 2b), and the mean error of the data in the 100 m bins (Fig. 2c). The resulting uncertainty of the tropospheric H₂O column density due to the experimental errors is $0.6 \cdot 10^{22}$ molec./cm² or approximately 6%. The variability of the data in the 100 m bins leads to an additional uncertainty of the column of about $0.3 \cdot 10^{22}$ molec./cm² or 3%.

Due to the lack of experimental H₂O data in the upper troposphere with H₂O mixing ratios below the Lyman-alpha detection limit of approximately 50–100 ppmV or ≈ 9 km the resulting H₂O column towards the tropopause at approximately 17 km altitude was estimated from a “range” of H₂O mixing ratios of (50 ± 50) ppmV to be about $(2 \pm 2) \cdot 10^{20}$ molec./cm². Since the tropospheric H₂O columns in the measurement area in this season are in the order of 10^{23} molec./cm² the contribution of the

upper tropospheric H₂O is well below 1% and can be neglected. The contribution of the stratospheric H₂O column is even smaller; according to the H₂O profile of the US standard atmosphere it is < 1‰.

2.2. GOME on ERS-2

5 The GOME instrument is one of several instruments aboard the European research satellite ERS-2 (European Space Agency (ESA), 1995). It consists of a set of four spectrometers that simultaneously measure sunlight reflected from the Earth's atmosphere and ground in four spectral windows covering the wavelength range between 240 and 790 nm with moderate spectral resolutions. The satellite operates in a nearly
10 polar, sun-synchronous orbit at an altitude of 780 km with an equator crossing time at approximately 1030 local time. While the satellite orbits in an almost north-south direction, the GOME instrument swaps in the perpendicular east-west direction. During one swap, three individual spectral scans are performed. The corresponding three ground pixels covering an area of 320 km from east to west by 40 km north to south lie side
15 by side giving a western, a centre, and an eastern pixel. The Earth's surface is totally covered within 3 days, and poleward from about 70° latitude within 1 day.

2.3. GOME analysis

The retrieval of the H₂O VCD from GOME measurements includes 2 basic steps. In the first step the integrated trace gas absorption along the light path which will also be referred to as the slant column density (SCD) is determined from the raw spectrum.
20 In the second step the SCD is transformed into the vertically integrated H₂O concentration, see e.g. Solomon et al. (1987).

2.3.1. Spectral retrieval

From the raw spectra (level 1 data) the trace gas absorption of H₂O as calculated
25 from the HITRAN data base (Rothman et al., 1992, 1998), and O₄ (Greenblatt et al.,

A fast H₂O total column density product from GOME

T. Wagner et al.

Title Page

Abstract

Introduction

Conclusions

References

Tables

Figures

◀

▶

◀

▶

Back

Close

Full Screen / Esc

Print Version

Interactive Discussion

A fast H₂O total column density product from GOME

T. Wagner et al.

[Title Page](#)[Abstract](#)[Introduction](#)[Conclusions](#)[References](#)[Tables](#)[Figures](#)[◀](#)[▶](#)[◀](#)[▶](#)[Back](#)[Close](#)[Full Screen / Esc](#)[Print Version](#)[Interactive Discussion](#)

© EGU 2003

1990) are analysed using the DOAS method (Platt, 1994). For this study the wavelength range from 612 to 676 nm was used. The measured spectra are modelled with a non-linear fitting routine (Stutz and Platt, 1996) that suitably weights the absorption spectra of the atmospheric trace gases including O₂ (Rothman et al., 1992, 1998) and a solar background spectrum (Fraunhofer reference spectrum). Also, the influence of atmospheric Raman scattering, the so-called Ring effect, is considered (Grainger and Ring, 1962; Bussemer, 1993). Contributions of atmospheric broad-band extinction processes (e.g. Rayleigh, and Mie scattering) and surface reflection are accounted for by including a third order polynomial into the fitting routine. The H₂O cross section was calculated for a fixed temperature and pressure of 273 K of 900 hPa, respectively. We therefore investigated the temperature and pressure dependence of the H₂O absorption structure by varying the temperature by ± 20 K and the pressure by ± 100 hPa. The analysis of GOME measurements using these different H₂O spectra yielded H₂O SCDs varying by only ± 3%. Compared to the other errors of the GOME H₂O analysis (see below) these uncertainties can be neglected.

From the inferred absorption, and the knowledge of the absorption cross section, the trace gas SCD is calculated. In Fig. 3 the result of the DOAS retrieval is shown. All three absorbers, H₂O, O₂ and O₄, respectively, can be clearly identified in the selected spectral window of the GOME spectrum. From the errors of the spectral fitting process and the uncertainty of the absorption cross section the total error of the derived atmospheric SCDs can be quantified (Stutz and Platt, 1996). For H₂O the error of the spectral retrieval is about 5% (or < 2 · 10²² molec./cm²). For O₄ the uncertainty is about 8% (or < 2 · 10⁴² molec.²/cm⁵. Here the O₄ column density is expressed as the integrated quadratic O₂ concentration, see Greenblatt et al., 1990). For the conversion of the observed O₄ absorption into the respective column density we applied an O₄ cross section of 9.61 · 10⁴⁶ cm⁵/molec² which was determined from atmospheric observations (Wagner et al., 2002). In some cases the relative fitting error of O₄ can become significantly larger than that of H₂O. This was found especially for large atmospheric H₂O columns over ocean surfaces, most probably due to the small light intensity over

the dark surface and/or the impact of sun glint.

2.3.2. Correction of the non-linearity between the measured absorption and the atmospheric H₂O column density

While the broad band O₄ absorptions can be spectrally resolved by the GOME instrument, this is not the case for the highly fine structured H₂O and O₂ absorption bands. Thus the derived H₂O SCD is no more a linear function of the atmospheric H₂O column density (Solomon et al., 1989; Wagner et al., 2000). Especially for large H₂O SCDs this effect can become important, e.g. for an atmospheric H₂O SCD of $2.5 \cdot 10^{23}$ molec./cm² the underestimation is about 30%. Nevertheless, a correction can be easily applied to the results of the DOAS analysis. The respective correction factors are calculated from the numerical simulation of this effect by mathematical convolution of the high resolved H₂O spectrum with the instruments slit function.

First, the spectrally high resolved H₂O cross section $\sigma(\lambda)$, taken from the HITRAN data base (Rothman, 1992, 1998), is multiplied with the assumed atmospheric H₂O SCD and the respective atmospheric absorption spectrum is calculated according to Beer-Lamberts law:

$$I(\lambda) = I_0(\lambda) \cdot \exp[-\sigma(\lambda) \cdot SCD]. \quad (1)$$

Second, this H₂O absorption spectrum is convoluted with the instrument response function of GOME $F(\lambda, \lambda')$:

$$I^*(\lambda) = F * I(\lambda) = \int F(\lambda\lambda') \cdot d\lambda'. \quad (2)$$

In the third step the logarithm is applied to the convoluted H₂O absorption spectrum which is then analysed using the DOAS method in the same way as for the real GOME measurements. In Fig. 4 the relationship between the derived H₂O SCD and the H₂O SCD which is used as the input for the modelling is shown. As indicated above, for

A fast H₂O total column density product from GOME

T. Wagner et al.

Title Page

Abstract

Introduction

Conclusions

References

Tables

Figures

◀

▶

◀

▶

Back

Close

Full Screen / Esc

Print Version

Interactive Discussion

small H₂O SCDs the non-linearity is still small, but large H₂O are systematically underestimated by up to more than 30%. Using this relationship the H₂O SCDs derived from the DOAS retrieval are corrected and the actual H₂O SCD is determined.

This approach combines the advantage of the fast and robust DOAS retrieval with the necessary correction for saturation effects in the spectra. In Fig. 5 (upper and middle panel) the impact of the saturation correction is demonstrated for one GOME orbit. For high H₂O SCDs in the tropics the largest correction has to be applied.

2.3.3. Application of “measured” air mass factors

Since the derived H₂O SCDs strongly depend on the solar zenith angle (SZA), they have to be converted into VCDs. Usually for this purpose the radiative transfer through the atmosphere is modelled, see e.g. Solomon et al. (1987), and Marquard et al. (2000). The results of these numerical models are conventionally expressed as air mass factors (AMF) which describe the ratio between the SCD and the VCD. However, while this is possible with high accuracy for stratospheric trace gases like NO₂ or O₃, the situation is much more complicated for tropospheric absorbers. Since the air density increases towards the surface multiple Rayleigh scattering plays an important role for tropospheric observations. Also, reflections at the ground further increase the effects of multiple scattering, especially for a large ground albedo. Finally, the influence of aerosols and in particular clouds becomes very important. In extreme cases, clouds can completely shield trace gases which are located below the cloud cover. For these reasons the numerical modelling of the radiative transfer through the troposphere may lead to large uncertainties (Richter and Burrows, 2002; Wagner et al., 2001). Even if detailed information on the different atmospheric and ground/surface properties within a GOME ground pixel was available (which is usually not the case) current radiative transfer models still have deficiencies in the adequate modelling of the radiative transfer inside clouds. This is why the application of “measured AMFs” becomes an interesting option. These “measured AMFs” can be derived from the absorptions of tropospheric gases with known (and almost constant) concentrations. The

A fast H₂O total column density product from GOME

T. Wagner et al.

Title Page

Abstract

Introduction

Conclusions

References

Tables

Figures

◀

▶

◀

▶

Back

Close

Full Screen / Esc

Print Version

Interactive Discussion

A fast H₂O total column density product from GOME

T. Wagner et al.

[Title Page](#)[Abstract](#)[Introduction](#)[Conclusions](#)[References](#)[Tables](#)[Figures](#)[◀](#)[▶](#)[◀](#)[▶](#)[Back](#)[Close](#)[Full Screen / Esc](#)[Print Version](#)[Interactive Discussion](#)

© EGU 2003

ratio between the measured SCD of such an absorber and the known VCD for a standard atmosphere, e.g. normal conditions at ground, clear sky, yields the “measured AMF”. Such “measured AMFs” automatically take into account the effects of multiple scattering, aerosols, ground albedo and clouds. It should be noted here that because of the large ground pixel size nearly all GOME observations are affected by clouds which thus are usually the dominant source of error for tropospheric observations (Richter and Burrows, 2002; Wagner et al., 2001; Velders et al., 2001).

First attempts towards “measured AMFs” were undertaken by Noël et al. (2000, 2002) and Casadio et al. (2000) utilizing measurements of the atmospheric O₂ absorption. Because of the large difference between the shapes of the concentration profiles of O₂ and H₂O, however, it is evident that the derived correction is usually not well suited for the application to the H₂O measurements. Let us assume for example a cloud at about 2 km altitude. While most of the H₂O absorption is shielded by this cloud (the bulk of the H₂O is located close to the ground), most of the O₂ column is still above the cloud. In this study we use the simultaneous measurements of O₄ for the determination of the “measured AMF”. Because of the square dependence of the O₄ concentration on the O₂ concentration (see e.g. Greenblatt et al., 1990) the dominant contribution of the O₄ profile is located much closer to the ground; the scale height is only about 4 km compared to 8 km for O₂ (see Fig. 1). Because of the larger similarity between the O₄ profile and the H₂O profile, the measured O₄ AMFs are therefore much more appropriate for the conversion of the measured H₂O SCDs into VCDs. However, the measured O₄ AMFs are also subject to several limitations:

First, the cloud correction is only valid under the assumption that the H₂O profile is horizontally homogeneous throughout the whole GOME ground pixel. This is in general not the case; especially for measurements with cloud fractions close to 100% the respective error can become large.

Second, because of the remaining difference of the H₂O and O₄ profiles and because of the differences in the absorption strengths the actual AMFs for both species still show systematic deviations. While for large SZA the difference in the profile shape

A fast H₂O total column density product from GOME

T. Wagner et al.

[Title Page](#)[Abstract](#)[Introduction](#)[Conclusions](#)[References](#)[Tables](#)[Figures](#)[◀](#)[▶](#)[◀](#)[▶](#)[Back](#)[Close](#)[Full Screen / Esc](#)[Print Version](#)[Interactive Discussion](#)

© EGU 2003

is the dominant effect, for small SZA the difference in the absorption strength becomes more important due to the high H₂O concentrations in the tropics where the smallest SZA for a GOME orbit appear. We modelled these effects using the Monte Carlo radiative transfer model AMFTRAN (Marquard et al., 2000) assuming clear sky conditions and a ground albedo of 5%. Both effects lead to a systematic underestimation of the actual H₂O SCD which ranges between about 16% in the tropics and about 18% for measurements at 80° SZA. For medium SZA, between about 40° and 70°, the underestimation is smallest (about 12%). It is important to note that for higher values of the ground albedo the differences become significantly smaller.

Third, due to the different profile shapes of H₂O and O₄ the effects of clouds are different for both species. We also modelled these effects with our radiative transfer model. We used the simplifying assumptions that clouds were reflecting surfaces with an albedo of 80%. Two dominant effects have to be considered:

A) The cloud shielding effect: Especially for low and medium high clouds the relative fraction of the total VCD which is shielded below the cloud is systematically different for both species. In contrast, this effect becomes negligible for high clouds, e.g. in the tropics, since then the main part of the total H₂O VCD as well as the main part of the total O₄ VCD is shielded. Also for surface near clouds or fog the errors are small. In Table 1 the magnitude of the underestimation of the GOME H₂O VCD is summarised.

B) The cloud albedo effect: Since clouds are bright they enhance the sensitivity towards trace gases directly above the cloud with respect to the clear sky scene with a low ground albedo (Richter and Burrows, 2002; Wagner et al., 2001; Velders et al., 2001).

Thus especially low clouds or fog at the ground can enhance the sensitivity of the measurements for H₂O. Thus they might to a small degree compensate the shielding effect of clouds. A similar but generally smaller effect can be also due to multiple Mie scattering inside the clouds or reflections between the cloud layer and the surface. Nevertheless, these effects should in general be small and the shielding effect is expected to dominate the total cloud effect.

Because of the above arguments in specific cases, the differences between the de-

A fast H₂O total column density product from GOMET. Wagner et al.

[Title Page](#)[Abstract](#)[Introduction](#)[Conclusions](#)[References](#)[Tables](#)[Figures](#)[◀](#)[▶](#)[◀](#)[▶](#)[Back](#)[Close](#)[Full Screen / Esc](#)[Print Version](#)[Interactive Discussion](#)

© EGU 2003

rived and the actual H₂O VCDs can become relatively large. However, for most of the measurements it can be expected to be in the order of <20% (underestimation of the actual H₂O VCD). However, these uncertainties have to be compared to the uncertainties which can appear if calculated AMFs are used and no or a not adequate cloud correction is applied or wrong aerosol and albedo data are used: Even for clear sky conditions the influence of a changing ground albedo and changing aerosol content can cause systematic errors of up to more than 30%. If the influence of clouds is not corrected, an additional systematic underestimation of the H₂O VCD in the order of about 50% or more can be expected for nearly all GOME observations, because nearly all GOME ground pixels are partly covered by clouds. These effects are directly corrected for by our method of 'measured AMFs'. In the lower panel of Fig. 5 the H₂O VCDs for the selected GOME orbit are shown. Especially in the tropics the strong variation of the H₂O SCDs (caused by clouds) is strongly reduced by the application of the "measured AMFs".

3. Results and discussion

3.1. Comparison of measured and modelled H₂O VCDs along one GOME orbit

In Fig. 6 the H₂O VCDs derived with our method for a selected GOME orbit (see Fig. 5) are displayed. The same orbit was also analysed by Maurellis et al. (2000), and Lang et al. (2002), who compared their data to model values from ECMWF. We used these modelled H₂O VCDs also for a comparison with our GOME H₂O analysis. The results of our study (here all measurements including the cloudy scenes are shown) agree well with the model results. In particular, the shielding effect of the clouds affects the derived H₂O VCDs around the latitude of 5° much less than in the data from Maurellis et al. (2000). Lang et al. (2002) found that their GOME H₂O results compare well with the ECMWF data only for cloud fractions <10%.

3.2. Comparison with in-situ aircraft data during MINOS 2001

During the MINOS campaign in Greece 2001 (Lelieveld et al., 2002, <http://www.mpch-mainz.mpg.de/~reus/minos/index.htm>) airborne in-situ H₂O observations were made which could be compared to tropospheric H₂O VCDs from GOME. In total, during the course of the campaign, seven flights do show a reasonably good temporal and spatial overlap with the GOME observations. However, because the aircraft missions were not optimised for satellite validation the flight tracks did not necessarily cover a representative area of a GOME ground pixel. Therefore, it should be noted that especially in cases of strong gradients or fluctuations of the H₂O VCD or other parameters like e.g. ground albedo or cloud cover across one or more GOME ground pixels, even for a good overlap the explanatory power of a comparison between GOME and aircraft observations is limited.

Because the atmospheric H₂O VCD is dominated by the contributions close to the ground only those GOME pixels covering the areas of a full vertical aircraft profile including the start and/or landing areas over Crete were selected for the comparisons.

For all comparisons the sky was almost cloud free according to METEOSAT images (Mannstein, 2002) and GOME cloud fractions as derived with the CRUSA cloud algorithm, see Wenig (2001). However, on some days, e.g. on 14 August 2001, several small cloud fragments were spread over the Mediterranean Sea.

An overview of all coincidences and a comparison of the respective H₂O columns derived from the measurements during the MINOS 2001 campaign are shown in Table 2 and Fig. 7. Generally, for the flights which were made close to the time of the GOME overpass the agreement between both, the GOME and in-situ data is very good. For instance, for MINOS flights # 5 and # 6 the agreement is excellent.

The result for flight # 7, which was made on the same day and in almost the same region as flight # 6, but approximately 7 h later, reveals a strong deviation which can be attributed to the large temporal difference.

Another case with only moderate agreement between the GOME (8.7·10²²

A fast H₂O total column density product from GOME

T. Wagner et al.

Title Page

Abstract

Introduction

Conclusions

References

Tables

Figures

◀

▶

◀

▶

Back

Close

Full Screen / Esc

Print Version

Interactive Discussion

A fast H₂O total column density product from GOME

T. Wagner et al.

[Title Page](#)[Abstract](#)[Introduction](#)[Conclusions](#)[References](#)[Tables](#)[Figures](#)[◀](#)[▶](#)[◀](#)[▶](#)[Back](#)[Close](#)[Full Screen / Esc](#)[Print Version](#)[Interactive Discussion](#)

© EGU 2003

molec./cm²) and the in-situ data ($6.8 \cdot 10^{22}$ molec./cm²) is MINOS flight # 10. On the day of this flight (19.08.2001) the GOME observations show a strong west-east gradient in the Falcon flight area, see Fig. 8. The boundary layer was sampled by the aircraft in the south-east part of the Falcon flight descending from the west into Heraklion, Crete.

5 With the assumption that the H₂O VCD east-west gradient of $5.5 \cdot 10^{22}$ molec./cm² per 650 km – as estimated from the three neighbouring GOME measurements – also exists across the eastern GOME pixel of the Falcon flight area a H₂O VCD of $7.3 \cdot 10^{22}$ molec./cm² is estimated over Crete. This value is very close to – and well within the error margins of – the H₂O column of $6.8 \cdot 10^{22}$ molec./cm² as determined from the aircraft

10 observations.

It can be concluded that the agreement between the GOME and in-situ columns is generally very good and the differences are mainly due to poor spatial and temporal coincidences, especially when strong gradients are observed in the area of interest.

4. Conclusions

15 A new and fast GOME algorithm for the retrieval of the total atmospheric column of H₂O was developed. In contrast to already existing algorithms no additional a-priori information on the climatic zone or other important parameters like atmospheric aerosol content, surface albedo or cloud cover is needed. It includes an internal cloud-, aerosol-, and albedo correction which is based on simultaneous observations of the oxygen dimer O₄.

20 Although a systematic underestimation of the H₂O VCD is to be expected because of the different atmospheric altitude profiles of H₂O and O₄, the resulting errors are small (between 12% and 18%) for clear sky conditions.

For GOME observations for an at least partly cloudy sky, the systematic underestimation of the derived H₂O VCD can become much larger than for cloud free conditions. This is because clouds shield different relative fractions of the H₂O and O₄ columns. Especially for large cloud fractions and low and medium high clouds the errors of a single observation can be up to more than 50%. Thus, in practice during routine operation

of this algorithm it might be reasonable to exclude H₂O VCDs for measurements with cloud fractions over a selected threshold. However, even for cloud fractions close to 100% the H₂O VCDs derived with our approach in the tropics showed good agreement with model results.

5 During the MINOS campaign in Greece in August 2001 GOME H₂O VCDs were compared to integrated H₂O altitude profiles from simultaneous aircraft observations. During these comparisons the sky was almost cloud free, and a good agreement between both observations was found confirming the small errors of the GOME H₂O VCD under clear sky conditions. Only for two days a larger difference was found, which can
10 in one case be attributed to a large horizontal gradient of H₂O and in the second to a large temporal difference between the aircraft measurement and the satellite overpass.

As mentioned above we expect that our GOME H₂O product systematically should underestimate the true H₂O column by about 12–18% for clear sky conditions. Thus the good agreement between the GOME and aircraft observations is somehow surprising.
15 One reason for this is that the underestimation is compensated by another effect. The most probable explanation is the temperature dependence of the O₄ absorption. We applied an O₄ cross section which was measured in polar winter, when the tropospheric temperatures is about 40 K lower than during the MINOS campaign (Wagner et al., 2002). The respective underestimation of the true atmospheric O₄ absorption at 630
20 nm is about 14% (Newnham and Ballard, 1998; Wagner et al., 2002). Thus this effect can nearly completely compensate the expected underestimation of the true H₂O VCD by GOME for a clear day.

It should be noted that our algorithm can be easily adapted to the nadir observations of SCIAMACHY which was launched on the European research satellite ENVISAT on
25 1 March 2002 (Bovensmann et al., 1999). Since there is already a large temporal overlap between GOME and SCIAMACHY we expect a continuous time series of the global atmospheric H₂O VCD over the entire lifetime of both sensors.

Acknowledgements. The authors thank M. Buchwitz, St. Noël, and A. Richter (University of Bremen, Germany) for interesting and constructive discussions.

A fast H₂O total column density product from GOME

T. Wagner et al.

Title Page

Abstract

Introduction

Conclusions

References

Tables

Figures

◀

▶

◀

▶

Back

Close

Full Screen / Esc

Print Version

Interactive Discussion

References

- Atkinson, R.: Gas-phase tropospheric chemistry of organic compounds: A review, *Atmospheric Environment*, 24A, 1–41, 1990.
- Atkinson, R.: Atmospheric chemistry of VOCs and NO_x, *Atmospheric Environment*, 34, 2063–2101, 2000.
- 5 Baltink, H. K., van der Marel, H., and van der Hoeven, A. G. A.: Integrated atmospheric water vapor estimates from a regional GPS network, *J. Geophys. Res.*, 107, D3, 4025, doi:10.1029/2000JD000094, 2002.
- Bauer, P. and Schuessel, P.: Rainfall, total water, ice water, and water vapor over sea-polarized microwave simulations and special sensor microwave/image data, *J. Geophys. Res.*, 98, 20737–20759, 1993.
- 10 Bevis, M., Businger, S., Herring, T. A., Rocken, C., Anthes, R. A., and Ware, R. H.: GPS meteorology: remote sensing of atmospheric water vapor using the global positioning system, *J. Geophys. Res.*, 97, 15787–15801, 1992.
- 15 Buck, A.: The Lyman-alpha absorption hygrometer, *ISA Proceedings of the International Symposium on Moisture and Humidity*, 411–436, 1985.
- Bovensmann, H., Burrows, J. P., Buchwitz, M., Frerik, J., Noël, S., Rozanov, V. V., Chance, K. V., and Goede, A.: SCIAMACHY – mission objectives and measurement modes, *J. Atmos. Sci.*, 56, 2, 127–150, 1999.
- 20 Bussemer, M.: *Der Ring-Effekt: Ursachen und Einfluß auf die spektroskopische Messung stratosphärischer Spurenstoffe*, Diploma thesis, University of Heidelberg, 1993.
- Casadio, S., Zehner, C., Pisacane, G., and Putz, E.: Empirical retrieval of the atmospheric air mass factor (ERA) for the measurement of water vapour vertical content using GOME data, *Geophys. Res. Lett.*, 27, 1483–1486, 2000.
- 25 Chaboureaud, J.-P., Chédin, A., and Scott, N. A.: Remote Sensing of the Vertical Distribution of Atmospheric Water Vapor from the TOVS Observations. Method and Validation, *J. Geophys. Res.*, 102, 4343–4352, 1997.
- European Space Agency (ESA): GOME, Global Ozone Monitoring Experiment, users manual, edited by F. Bednarz, Spec. Publ. SP-1182, Publ. Div. Eur. Space Res. and Technol. Cent. (ESTEC), Frascati, Italy, 1995.
- 30 Grainger, J. F. and Ring, J.: Anomalous Fraunhofer line profiles, *Nature*, 193, 762, 1962.
- Greenblatt G. D., Orlando, J. J., Burkholder, J. B., and Ravishankara, A. R.: Absorption

A fast H₂O total column density product from GOME

T. Wagner et al.

Title Page

Abstract

Introduction

Conclusions

References

Tables

Figures

◀

▶

◀

▶

Back

Close

Full Screen / Esc

Print Version

Interactive Discussion

measurements of oxygen between 330 and 1140 nm, *J. Geophys. Res.*, 95, 18577–18582, 1990.

5 Halthore, R. N., Eck, T. F., Holben, B. N., and Markham, B. L.: Sun photometric measurements of atmospheric water vapor column abundance in the 940-nm band, *J. Geophys. Res.*, 102, 4343–4352, 1997.

Helten, M., Smit, H. G. J., Sträter, W., Kley, D., Nedelec, P., Zöger, M., and Busen, R.: Calibration and performance of automatic compact instrumentation for the measurement of relative humidity from passenger aircraft, *J. Geophys. Res.*, 103, 25643–25652, 1998.

10 Jedlovec, G. J.: An evaluation and comparison of vertical profile data from the VISSR Atmospheric Sounder (VAS), *J. Atmos. Oceanic Technol.*, 2, 559–581, 1985.

Kley, D. and Russel, J. M.: SPARC assessment of upper tropospheric and stratospheric water vapour, edited by the SPARC office, Service d'Aéronomie, CNRS, Verrières-le-Buisson cedex, France, SPARC Newsletter n° 16, 11–16, 2001.

15 Lang, R., Williams, J. E., van der Zande, W. J., and Maurellis, A. N.: Application of the Spectral Structure Parameterization technique: retrieval of total water vapour columns from GOME, *Atmos. Chem. Phys. Discuss.*, 2, 1097–1130, 2002.

Lelieveld, J., Berresheim, H., Borrmann, S., Crutzen, P. J., Dentener, F. J., Fischer, H., de Gouw, J., Feichter, J., Flatau, P., Heland, J., Holzinger, R., Kormann, R., Lawrence, M., Levin, Z., Markowicz, K., Mihalopoulos, N., Minikin, A., Ramanathan, V., de Reus, M., Roelofs, G. J., Scheeren, H. A., Sciare, J., Schlager, H., Schultz, M., Siegmund, P., Steil, B., Stier, P., Traub, M., Warneke, C., Williams, J., and Ziereis, H., *Global air pollution crossroads over the Mediterranean*, *Science*, 298, 794-799, 2002.

Mannstein, H.: DLR-IPA, Germany, personal communication 2002.

25 Marquard, L. C., Wagner, T., and Platt, U.: Improved air mass factor concepts for scattered radiation differential optical absorption spectroscopy of atmospheric species, *J. Geophys. Res.*, 105, 1315–1327, 2000 .

Maurellis, A. N., Lang, R., van der Zande, W. J., Aben, I., and Ubachs, W.: Precipitable Water Column Retrieval from GOME data, *Geophys. Res. Lett.*, 27, 903–906, 2000.

Newnham, D. A. and Ballard, J.: Visible absorption cross section and integrated absorption intensities of molecular oxygen (O₂ and O₄), *J. Geophys. Res.*, 103, 28801–28816, 1998.

30 Noël, S., Buchwitz, M., Bovensmann, H., Hoogen, R., and Burrows, J. P.: Atmospheric Water Vapor Amounts Retrieved from GOME Satellite data, *Geophys. Res. Lett.*, 26, 1841–1844, 1999.

A fast H₂O total column density product from GOME

T. Wagner et al.

Title Page

Abstract

Introduction

Conclusions

References

Tables

Figures

◀

▶

◀

▶

Back

Close

Full Screen / Esc

Print Version

Interactive Discussion

A fast H₂O total column density product from GOME

T. Wagner et al.

[Title Page](#)[Abstract](#)[Introduction](#)[Conclusions](#)[References](#)[Tables](#)[Figures](#)[◀](#)[▶](#)[◀](#)[▶](#)[Back](#)[Close](#)[Full Screen / Esc](#)[Print Version](#)[Interactive Discussion](#)

© EGU 2003

- Noël, S., Bovensmann, H., and Burrows, J. P.: Water vapour retrieval from GOME data including cloudy scenes, Proc. ENVISAT/ERS Symposium, Gothenburg, 2000.
- Noël, S., Buchwitz, M., Bovensmann, H., and Burrows, J. P.: Retrieval of Total Water Vapour Column Amounts from GOME/ERS-2 Data, Adv. Space Res., 29, 1697–1702, 2002.
- 5 Platt, U.: Differential optical absorption spectroscopy (DOAS), in Air Monitoring by Spectroscopic Techniques, M. W. Sigrist (Ed.), Chemical Analysis Series Vol. 127, John Wiley, New York, 1994.
- Richter, A. and Burrows, J. P.: Retrieval of Tropospheric NO₂ from GOME Measurements, Adv. Space Res., 29, 11, 1673–1683, 2002.
- 10 Rocken, C., Hove, T. V., and Ware, R.: Near real-time GPS sensing of atmospheric water vapor, Geophys. Res. Lett., 24, 3221–3224, 1997.
- Rothman, L. S., Gamache, R. R., Tipping, R. H., Rinsland, C. P., Smith, M. A. H., Benner, D. C., Malathy Devi, V., Flaud, J.-M., Camy-Peyret, C., Perrin, A., Goldman, A., Massie, S. T., Brown, L. R., and Toth, R. A.: The HITRAN molecular database: editions of 1991 and 1992, 15 J. Quant. Spectrosc. Radiat. Transfer, 48, 5/6, 469–508, 1992.
- Rothman, L. S., Rinsland, C. P., Goldman, A., Massie, S. T., Edwards, D. P., Flaud, J.-M., Perrin, A., Camy-Peyret, C., Dana, V., Mandin, J.-Y., Schroeder, J., McCann, A., Gamache, R. R., Wattson, R. B., Yoshino, K., Chance, K. V., Jucks, K. W., Brown, L. R., Nemtchinov, V.; and Varanasi, P.: The HITRAN molecular spectroscopic database and HAWKS (HITRAN 20 Atmospheric Workstation): 1996 edition, Journal of Quantitative Spectroscopy and Radiative 20 Transfer, 60, 5, 665–710, 1998.
- Schaeler, B. and Riese, M.: Retrieval of Water Vapor in the Tropopause Region from CRISTA Measurements, Adv. Space Res., 27, 1635–1640, 2001.
- Soden, B. J. and Bretherton, F. P.: Interpretation of TOVS water vapor radiances in terms of layer-average relative humidities: Method and climatology for the upper, middle, and lower 25 troposphere, J. Geophys. Res., 101, 9333–9343, 1996.
- Solomon, S., Schmeltekopf, A. L., and Sanders, R. W.: On the interpretation of zenith sky absorption measurements, J. Geophys. Res., 92, 8311–8319, 1987.
- Solomon, S., Miller, H. L., Smith, J. P., Sanders, R. W., Mount, G. H., Schmeltekopf, A. L., and Noxon, J. F.: Atmospheric NO₃. 1. Measurement Technique and the Annual Cycle, J. 30 Geophys. Res., 94, 11041–11048, 1989.
- Ström, J., Busen, R., Quante, M., Guillemet, B., Brown, P. R. A., and Heintzenberg, J.: Pre-EUCREX intercomparison of airborne humidity measuring instruments, J. Atmos. Oceanic

A fast H₂O total column density product from GOME

T. Wagner et al.

[Title Page](#)[Abstract](#)[Introduction](#)[Conclusions](#)[References](#)[Tables](#)[Figures](#)[◀](#)[▶](#)[◀](#)[▶](#)[Back](#)[Close](#)[Full Screen / Esc](#)[Print Version](#)[Interactive Discussion](#)

© EGU 2003

Techn., 11, 1392–1399, 1994.

Stutz, J. and Platt, U.: Numerical analysis and error estimation of Differential Optical Absorption Spectroscopy measurements least-squares methods, *Appl. Optics*, 35, 6041–6053, 1996.

Van Roozendael, M., Fayt, C., Lambert, J.-C., Pundt, I., Wagner, T., Richter, A., and Chance, K.: Development of a bromine oxide product from GOME, in *Proceedings of the European Symposium on Atmospheric Measurements From Space (ESAMS 99)*, 18 to 22 Jan., ESTEC, Noordwijk, Netherlands, Eur. Space Agency, Noordwijk, Netherlands, Rep. WPP-161, 543–547, 1999.

Velders, G. J. M., Granier, C., Portmann, R. W., Pfeilsticker, K., Wenig, M., Wagner, T., Platt, U., Richter, A., and Burrows, J. P.: Global tropospheric NO₂ column distributions: Comparing 3-D model calculations with GOME measurements, *J. Geophys. Res.*, 106, 12643–12660, 2001.

Wagner, T., Otten, C., Pfeilsticker, K., Pundt, I., and Platt, U.: DOAS moonlight observation of atmospheric NO₃ and NO₂ in the Arctic winter, *Geophys. Res. Lett.*, 27, 3441–3444, 2000.

Wagner, T., Leue, C., Wenig, M., Pfeilsticker, K., and Platt, U.: Spatial and temporal distribution of enhanced boundary layer BrO concentrations measured by the GOME instrument aboard ERS-2, *J. Geophys. Res.*, 106, 24225–24236, 2001.

Wagner, T., von Friedeburg, C., Wenig, M., Otten, C., and Platt, U.: UV/vis observations of atmospheric O₄ absorptions using direct moon light and zenith scattered sunlight for clear and cloudy sky conditions, *J. Geophys. Res.*, 107, D20, 4424, doi:10.1029/2001JD001026, 2002.

Wenig, M.: *Satellite Measurement of Long-Term Tropospheric Trace Gas Distributions and Source Strengths – Algorithm Development and Data Analysis*, PhD-Thesis, University of Heidelberg, Germany, 2001.

Wickert, J., Reigber, C., Beyerle, G., König, R., Marquard, C., Schmidt, T., Grunwaldt, L., Galas, R., Meehan, T. K., Melbourne, W. G., and Hocke, K.: Atmospheric sounding by GPS radio occultation: first results from CHAMP, *Geophys. Res. Lett.*, 28, 3263–3266, 2001.

Zöger, M., Afchine, A., Eicke, N., Gerhards, M.-T., Klein, E., McKenna, D. S., Mörschel, U., Schmidt, U., Tan, V., Tuitjer, F., Woyke, T., and Schiller, C.: Fast in-situ stratospheric hygrometers: A new family of balloon-borne and airborne Lyman α photofragment fluorescence hygrometers, *J. Geophys. Res.*, 104, D1, 1807–1816, 1999.

A fast H₂O total column density product from GOME

T. Wagner et al.

Table 1. Estimated underestimation of the H₂O VCD in the case of partially cloudy GOME ground pixels. For the calculations it is assumed that clouds are shielding surfaces with an albedo of 80%. The errors are largest for clouds between 1 and 5 km altitude

Cloud top height	Cloud fraction 20%	Cloud fraction 50%	Cloud fraction 70%
<1 km	< 5%	< 15%	< 30%
1–5 km	<10%	< 25%	< 45%
5–8 km	< 8%	< 20%	< 35%
> 8 km	< 3%	< 6%	< 15%

Title Page

Abstract

Introduction

Conclusions

References

Tables

Figures

◀

▶

◀

▶

Back

Close

Full Screen / Esc

Print Version

Interactive Discussion

© EGU 2003

A fast H₂O total column density product from GOME

T. Wagner et al.

Table 2. Overview of all coincidences and a comparison of the respective H₂O columns derived from the measurements during the MINOS 2001 campaign

Flight No. (Date)	in-situ H ₂ O VCD 10 ²² molec./cm ² (time of flight, UTC)	GOME H ₂ O VCD 10 ²² molec./cm ² (time of overpass, UTC)	cloud cover	Notes
#5 (12 Aug. 2001)	8.0 (11:00–14:30)	8.0 (09:55)	almost cloud free	small spatial overlap
#6 (14 Aug. 2001)	10.1 (07:20–08:40)	10.2 (08:52)	a new small clouds	very small region
#7 (14 Aug. 2001)	7.7 (14:15–15:20)	11.0 (08:52)	few small clouds	large time difference (> 5 h)
#8 (16 Aug. 2001)	9.3 (13:30–14:30)	8.8 (09:29)	cloud free	large time difference (> 4 h)
#9 (17 Aug. 2001)	8.3 (13:10–14:30)	8.6 (08:58)	almost cloud free	large spatial gradients in GOME data, large time difference (> 4 h)
# 10 (19 Aug. 2001)	6.8 (10:00–11:00)	8.7 (08:58)	a few small clouds	large spatial gradients in GOME data
#11 (19 Aug. 2001)	8.5 (13:30–16:45)	8.5 (08:58)	a few small clouds	large time difference (> 4 h)

[Title Page](#)
[Abstract](#)
[Introduction](#)
[Conclusions](#)
[References](#)
[Tables](#)
[Figures](#)
[Back](#)
[Close](#)
[Full Screen / Esc](#)
[Print Version](#)
[Interactive Discussion](#)

A fast H₂O total column density product from GOME

T. Wagner et al.

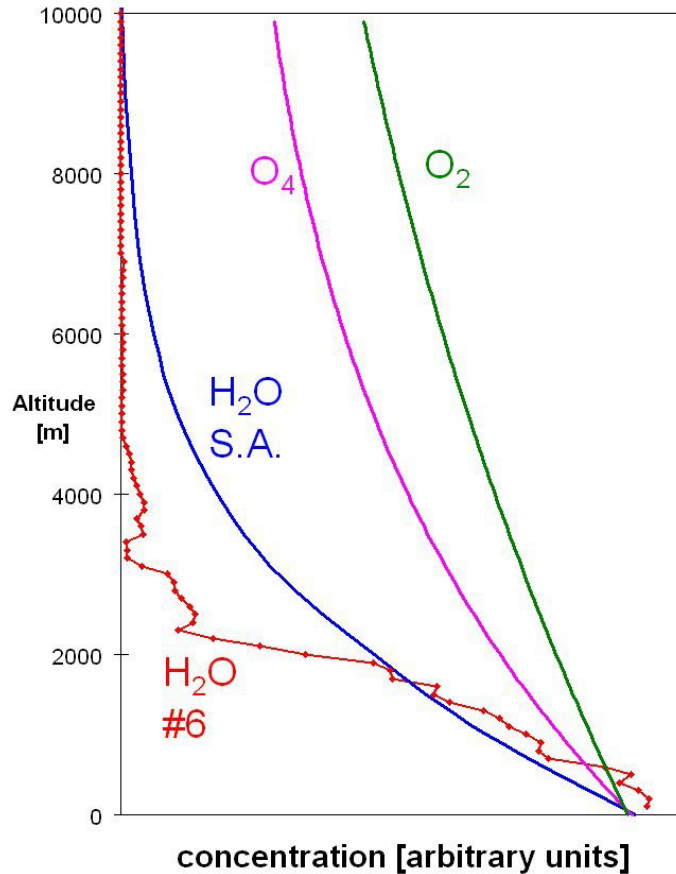


Fig. 1. Atmospheric height profiles for H₂O, O₂, and O₄. The bulk of the atmospheric O₄ column is located much closer to the earth's surface than that for O₂ ("H₂O SA" indicates the H₂O profile of the 1976 US standard atmosphere, "H₂O #6" that of the MINOS flight #6, see also Fig. 2).

[Title Page](#)[Abstract](#)[Introduction](#)[Conclusions](#)[References](#)[Tables](#)[Figures](#)[◀](#)[▶](#)[◀](#)[▶](#)[Back](#)[Close](#)[Full Screen / Esc](#)[Print Version](#)[Interactive Discussion](#)

© EGU 2003

A fast H₂O total column density product from GOME

T. Wagner et al.

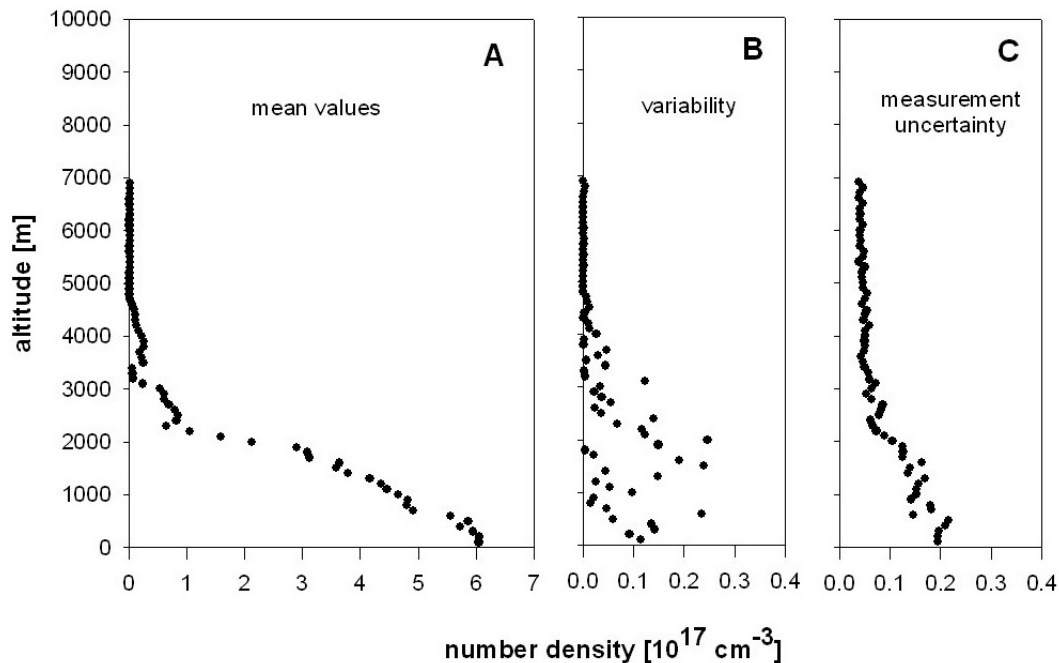


Fig. 2. Falcon H₂O measurements as a function of altitude (A) on MINOS flight #6 (14 August 2001) between 07:20–08:40 TUC including the variability of the experimental data in the 100 m altitude bins (B) and the measurement errors (C).

[Title Page](#)[Abstract](#)[Introduction](#)[Conclusions](#)[References](#)[Tables](#)[Figures](#)[◀](#)[▶](#)[◀](#)[▶](#)[Back](#)[Close](#)[Full Screen / Esc](#)[Print Version](#)[Interactive Discussion](#)

© EGU 2003

A fast H₂O total column density product from GOME

T. Wagner et al.

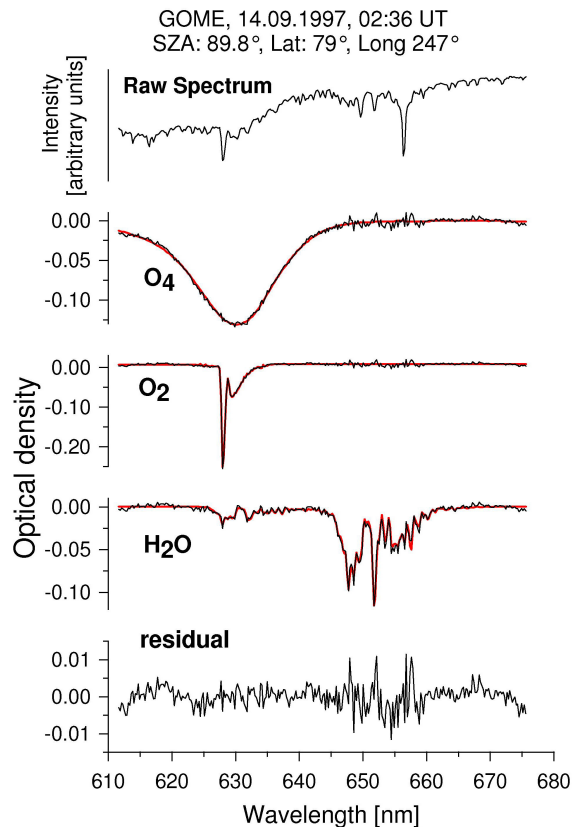


Fig. 3. In the upper panel a raw spectrum measured by GOME for the wavelength range of the H₂O analysis is shown. Below the results of the spectral evaluation for H₂O and O₄ for this GOME spectrum are presented. Also the result of the simultaneously analysed O₂ are included. The thick lines show the trace gas absorption spectra scaled to the respective absorptions detected in the measured GOME spectrum (thin lines).

[Title Page](#)[Abstract](#)[Introduction](#)[Conclusions](#)[References](#)[Tables](#)[Figures](#)[◀](#)[▶](#)[◀](#)[▶](#)[Back](#)[Close](#)[Full Screen / Esc](#)[Print Version](#)[Interactive Discussion](#)

© EGU 2003

A fast H₂O total column density product from GOME

T. Wagner et al.

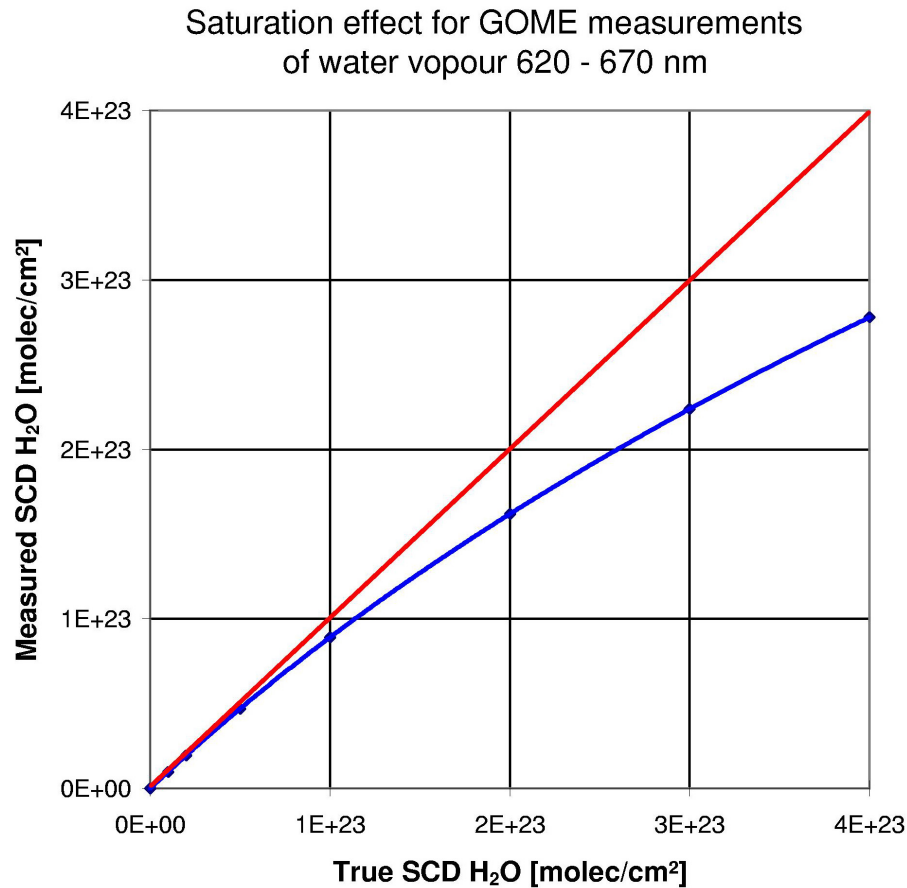


Fig. 4. Results of the numerical Simulation of the saturation effect of the H₂O measurements (at 650 nm) from GOME. The non-linearity between the actual H₂O VCD and the observed H₂O VCD from the DOAS analysis is indicated by the blue line.

[Title Page](#)[Abstract](#)[Introduction](#)[Conclusions](#)[References](#)[Tables](#)[Figures](#)[◀](#)[▶](#)[◀](#)[▶](#)[Back](#)[Close](#)[Full Screen / Esc](#)[Print Version](#)[Interactive Discussion](#)

© EGU 2003

A fast H₂O total column density product from GOME

T. Wagner et al.

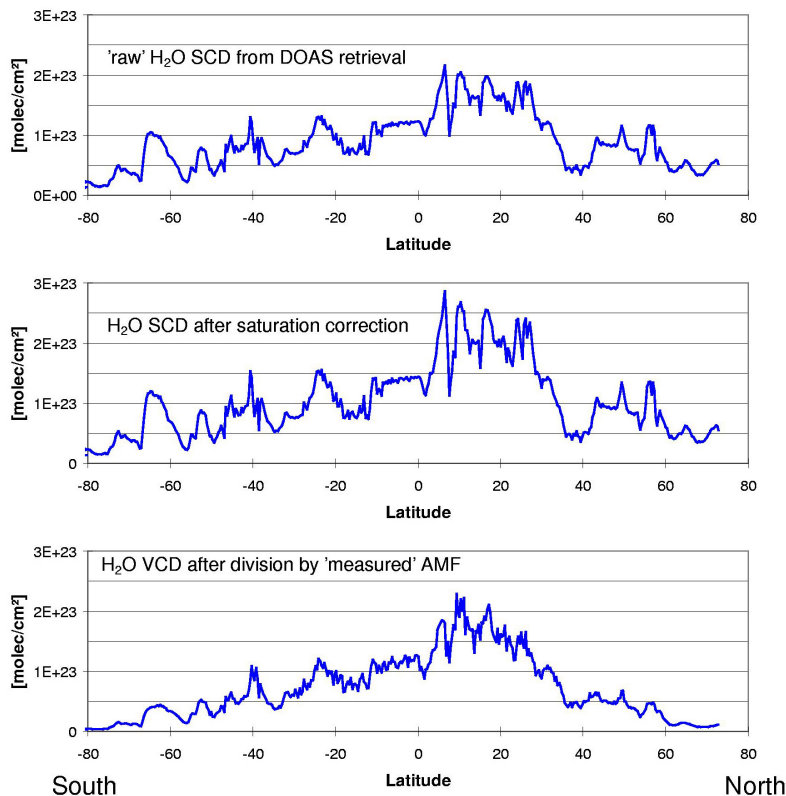


Fig. 5. Different steps of the GOME H₂O retrieval (for the orbit 81023175, 23 October 1998). Upper panel: the uncorrected H₂O SCDs as derived from the DOAS retrieval. Middle panel: H₂O SCDs after the correction of the “saturation effect” (see text). Lower panel: H₂O VCDs after application of the “measured AMFs”. It can be seen that the strong variations of the H₂O SCD between 0 and 30° latitude are strongly reduced after the conversion into the H₂O VCDs. This shows the power of our method in automatically correcting the influence of clouds.

[Title Page](#)[Abstract](#)[Introduction](#)[Conclusions](#)[References](#)[Tables](#)[Figures](#)[◀](#)[▶](#)[◀](#)[▶](#)[Back](#)[Close](#)[Full Screen / Esc](#)[Print Version](#)[Interactive Discussion](#)

A fast H₂O total column density product from GOME

T. Wagner et al.

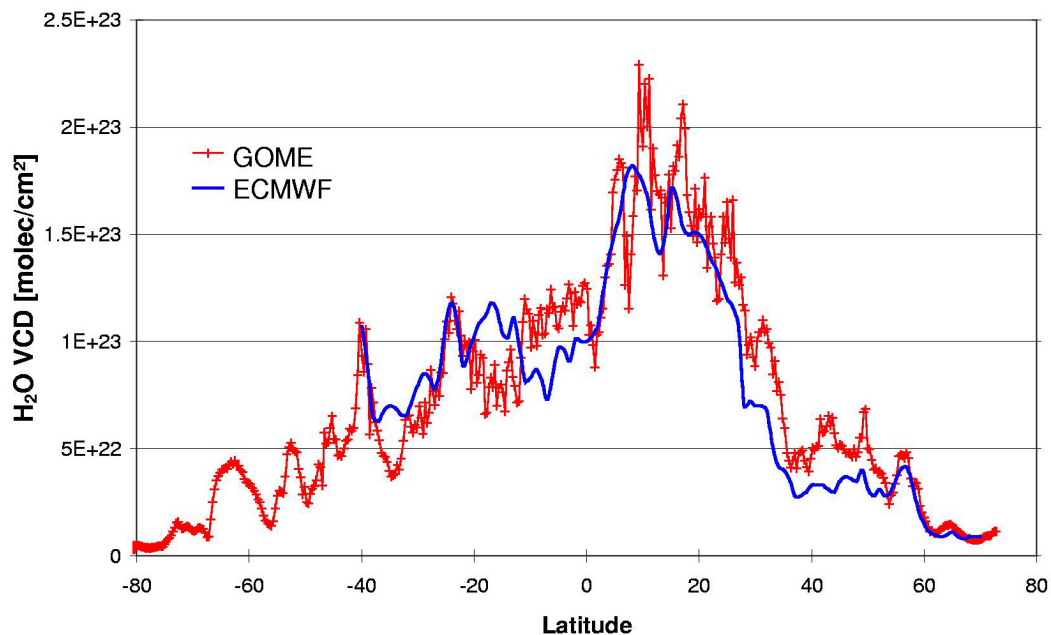


Fig. 6. Comparison of the GOME H₂O analysis for the same orbit as in Fig. 5 with modelled H₂O VCDs (ECMWF). The same orbit was also analysed by Maurellis et al. (2000) (from whom the model data are taken) and Lang et al. (2002).

[Title Page](#)[Abstract](#)[Introduction](#)[Conclusions](#)[References](#)[Tables](#)[Figures](#)[◀](#)[▶](#)[◀](#)[▶](#)[Back](#)[Close](#)[Full Screen / Esc](#)[Print Version](#)[Interactive Discussion](#)

© EGU 2003

A fast H₂O total column density product from GOME

T. Wagner et al.

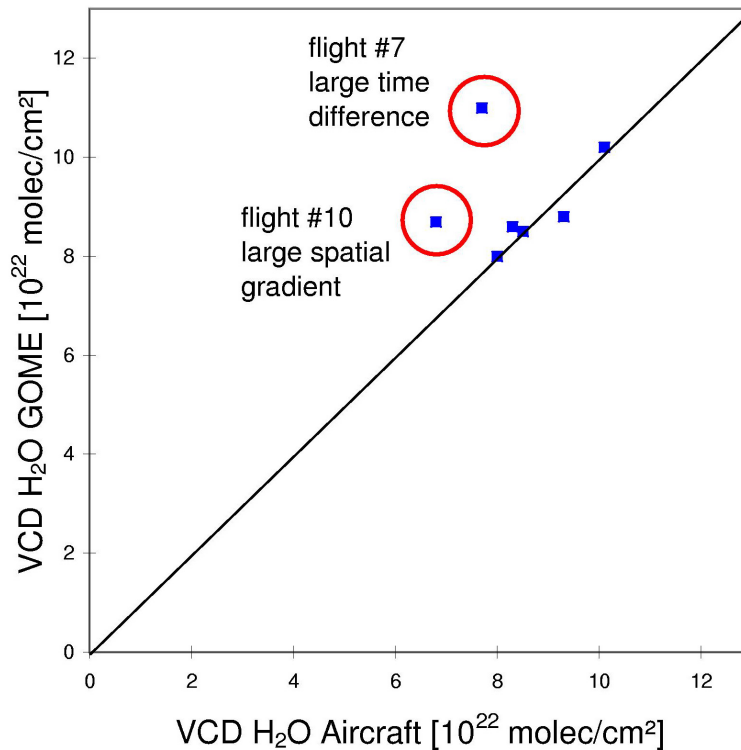


Fig. 7. Comparison between the H₂O VCD derived from the aircraft (x-axis) and satellite (y-axis). For the cases of good temporal and spatial coincidence good agreement is found. For some cases with a large temporal difference or large spatial gradients the agreement is worse (indicated by red circles).

[Title Page](#)[Abstract](#)[Introduction](#)[Conclusions](#)[References](#)[Tables](#)[Figures](#)[◀](#)[▶](#)[◀](#)[▶](#)[Back](#)[Close](#)[Full Screen / Esc](#)[Print Version](#)[Interactive Discussion](#)

© EGU 2003

A fast H₂O total column density product from GOME

T. Wagner et al.

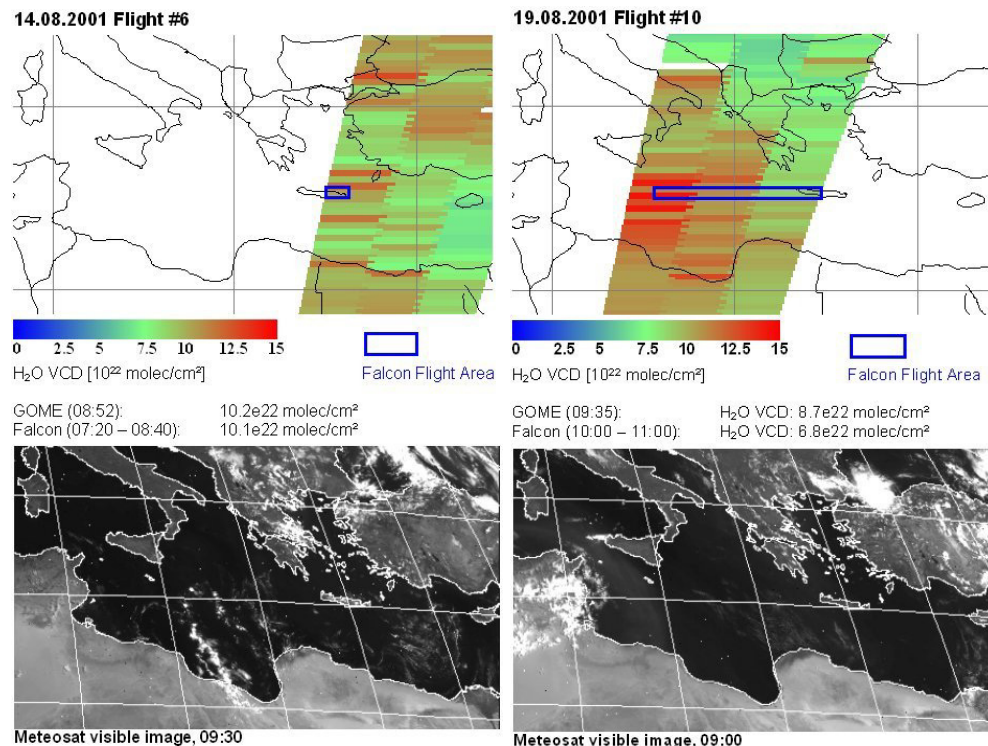


Fig. 8. GOME H₂O maps over the Mediterranean for 14 July (flight #6) and 19 July (flight #10). Also shown are satellite images from METEOSAT (Mannstein, 2002). For flight #6 an excellent agreement between the GOME and Falcon observations is found. For flight #10 both observations differ by about 30%. This discrepancy can be attributed to the strong west-east gradient of the H₂O VCD on that day (see text). For both flights (especially for flight #6) significant 'scatter' is found for the GOME H₂O data along the orbit. This scatter can be attributed to several small clouds over the Mediterranean Sea.

Title Page

Abstract

Introduction

Conclusions

References

Tables

Figures

◀

▶

◀

▶

Back

Close

Full Screen / Esc

Print Version

Interactive Discussion